

FRACTAL ANTENNA FOR PASSIVE UHF RFID APPLICATIONS

S. H. Zainud-Deen, H. A. Malhat, and K. H. Awadalla

Faculty of Electronic Engineering
Menoufia University
Egypt

Abstract—This paper addresses the design of fractal antennas placed onto dielectric object in the UHF RFID band and introduces a tag antenna configuration of simple geometry having impedance tuning capability. Through the paper, the dimensions of the fractal antenna are optimized to improve the impedance matching with the chip impedance. The tag performance changes are studied when it is placed on different objects (e.g., cardboard boxes with various content), or when other objects are present in the vicinity of the tagged object. It has been shown that a tag antenna can be designed or tuned for optimum performance on a particular object. Using the finite element method the open circuit voltage and the polarization mismatch factor against the operating frequency are calculated. The input impedance, reflection coefficient, power transmission coefficient and the read range as a function of frequency are illustrated. The performance of the tag antenna in the presence of the dielectric box and different object materials inside the box is illustrated. The effect of the objects that are placed in the center of the dielectric box didn't have a significant effect on the performance of the tag antenna; there is a small shift in the resonance frequency but still within the operating frequency band. Both the power transmission coefficient and the read range change with the object material. The backscattering properties of the tag antenna have been studied. The differential radar cross-section of the tag antenna is calculated for different antenna loads.

1. INTRODUCTION

The radio frequency identification (RFID) system is an automatic identification system using radio frequency waves to transfer data between reader units and movable objects called a transponder or tag. The RFID tag can be attached to almost anything such as pallets or cases of a product, documents, electronic devices, luggage, people, or pets in order to identify, track, or categorize them. The RFID tag consists of an electronic microchip and an antenna element. In general RFID tags can be categorized as active and passive. The active tags get their energy completely or partially from an integrated power supply, i.e., battery, while the passive tags do not have any power supply and rely only on the power extracted from the radio frequency signal transmitted by the reader. RFID tag antenna is loaded with the chip whose impedance switches between two impedance states, usually high and low. At each impedance state, RFID tag presents a certain radar cross section (RCS). The tag sends the information back by varying its input impedance and thus modulating the backscattered signal.

An antenna for an RFID-tag should satisfy the following requirements: 1) the antenna element should be thin; 2) it should be flexible with a simple shape; 3) the impedance bandwidth should be wide; 4) the antenna should provide omni-directional radiation pattern [1]. Different from the traditional antennas working at the resonant frequency, the conjugate matching method is used to design RFID antennas to get efficient power exchange between an antenna and a chip. The variation of the chip impedance with power and frequency can drastically affect the performance of the tag. Usually, in order to maximize the tag range, the antenna impedance is matched to the chip impedance at the minimum power level required for the chip to work. Conventional general-purpose tags are designed in free space, but when on-body applications are required, the strong pattern distortion and the efficiency loss, caused by the object dissipation and scattering, need to be taken into account in the first stage of the design. The presence of the object with its permittivity will induce strong power absorption with respect to free space.

Several papers have been published on RFID antennas for both passive and active tags, including covered slot antenna design [2], circular patch antenna analysis [3], meander antenna optimization [4], planar inverted F-antenna [5], folded dipole antenna [6], etc. however, very few papers [7–10] provided an overview of criteria for RFID tag antenna design and an analysis of practical application aspect.

RFID tag antennas tend to be too complicated for analytical solution as they can be used in complex environment. Tag antennas are

usually analyzed with electromagnetic modeling and simulation tools, typically with method of moments (MoM) for planar designs (e.g., thin flexible tags) and with finite-element method (FEM) or finite-difference time-domain method (FDTD) for more complicated three-dimensional designs (e.g., thick metal mounted tags). Tag antenna is first modeled, simulated, and optimized on a computer by monitoring the tag range, antenna gain, and impedance which give to a designer a good understanding of the antenna behavior.

Because of the size and tunability requirements, fractal antenna was a natural choice. Fractalizing allowed the antenna to be compact and matched with the chip impedance in the RFID frequency range and to provide omnidirectional performance in the plane perpendicular to the axis of the antenna. The performance of modified Koch fractal monopole antenna is compared to that of the meander line in [11]. It has been demonstrated that the less complex and less constrained geometries of the meander line are more effective at lowering resonant frequency than the Koch fractal monopole. A loaded meander antenna design for RFID application is demonstrated in [12]. In this paper, modified Koch fractal tag antenna mounted on a dielectric box containing different objects is investigated using the finite-element method. The design of the antenna has been conducted taking into account the presence of the dielectric box and its contents. The antenna input impedance is designed for conjugate-matching to high capacitive input impedance commercial UHF integrated microchip (IC) EPC Gen 2 RFID IC chip without using a loading bar as in [12]. The chip impedance is $Z_c = 40 - j133 \Omega$ at 930 MHz [13, 14]. The radiation properties of the antenna design are analyzed. The three design goals considered were a suitable impedance bandwidth, omnidirectional radiation pattern and simple structure.

The paper is organized as follows: the design of the modified Koch fractal antenna is presented first followed by the simulation method, FEM, and the simulation results of the antenna's return loss vs. frequency, the radiation patterns, the read range and gain. Finally the conclusion is presented.

2. FRACTAL ANTENNA; STRUCTURE AND ANALYSIS

Fractal antennas are characterized by their special geometric characteristics, which allow a reduction of the antenna dimensions [15, 16]. The geometry of the fractal monopole for the passive tag is shown in Figure 1. The values $s_1 = s_4$ equal to one third of the height L_a and change the angle α , scaling the values of $s_2 = s_3$ in order to preserve the height L_a constant for all iterations. In this case, the total de-

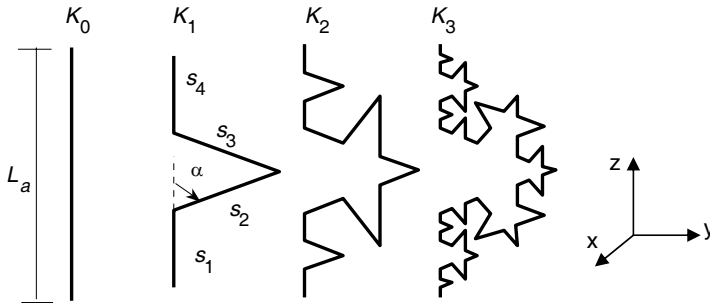


Figure 1. Curves correspondent to the four first iterations of the modified Koch fractal monopoles. K_0 and K_1 are initiator and generator, respectively for $\alpha = 70^\circ$.

ployed antenna length will increase with the number of iteration. This leads to a change of geometry and of the fractal dimension. Four affinity transformations W_1 , W_2 , W_3 and W_4 can be applied successively to construct the monopoles K_1 , K_2 , \dots , K_n . The procedure can be represented symbolically by [14]

$$K_{n+1} = \bigcup_{p=1}^4 W_p(K_n) = W_1(K_n) \cup W_2(K_n) \cup W_3(K_n) \cup W_4(K_n) \quad (1)$$

where n is the n th fractal iteration. The transformations are defined by the following expressions [16],

$$\begin{aligned} W_1 \begin{pmatrix} z_{n+1} \\ y_{n+1} \end{pmatrix} &= \begin{bmatrix} L_a/3 & 0 \\ 0 & L_a/3 \end{bmatrix} \begin{bmatrix} z_n \\ y_n \end{bmatrix} \\ W_2 \begin{pmatrix} z_{n+1} \\ y_{n+1} \end{pmatrix} &= \begin{bmatrix} (L_a/e_1) \cos \alpha & -(L_a/e_1) \sin \alpha \\ (L_a/e_1) \sin \alpha & (L_a/e_1) \cos \alpha \end{bmatrix} \begin{bmatrix} z_n \\ y_n \end{bmatrix} \\ &+ \begin{bmatrix} L_a/3 \\ 0 \end{bmatrix} \\ W_3 \begin{pmatrix} z_{n+1} \\ y_{n+1} \end{pmatrix} &= \begin{bmatrix} (L_a/e_1) \cos \alpha & (L_a/e_1) \sin \alpha \\ -(L_a/e_1) \sin \alpha & (L_a/e_1) \cos \alpha \end{bmatrix} \begin{bmatrix} z_n \\ y_n \end{bmatrix} \\ &+ \begin{bmatrix} L_a/2 \\ (L_a/6) \tan \alpha \end{bmatrix} \quad \text{and} \\ W_4 \begin{pmatrix} z_{n+1} \\ y_{n+1} \end{pmatrix} &= \begin{bmatrix} L_a/3 & 0 \\ 0 & L_a/3 \end{bmatrix} \begin{bmatrix} z_n \\ y_n \end{bmatrix} + \begin{bmatrix} 2L_a/3 \\ 0 \end{bmatrix} \end{aligned} \quad (2)$$

where $\epsilon_1 = 6 \cos \alpha$, The dimensions of antenna and iterations of the modified fractal antenna are optimized to improve the impedance matching with the chip impedance with smaller lengths. Throughout this paper only the 3rd-iteration modified fractal antenna K_3 is considered.

The polarization properties of the modified Koch fractal antenna may be accounted for by using complex vector effective length parameter \bar{h} to describe the receiving properties of an antenna. If \bar{E}^i is the incident electric field then \bar{h} is defined in such a way that the received open-circuit voltage is given by

$$V_{oc} = \bar{h} \cdot \bar{E}^i \tag{3}$$

where

$$\bar{h} = h_\theta \hat{a}_\theta + h_\phi \hat{a}_\phi \tag{4}$$

and

$$\bar{E}^i = E_\theta^i \hat{a}_\theta + E_\phi^i \hat{a}_\phi \tag{5}$$

The complex vector effective length is given by [17, 18]

$$h_i(\theta, \phi) = -\hat{a}_i \cdot \int \frac{\bar{I}(r')}{I_o} e^{jkr' \cos \gamma} dr' \tag{6}$$

where $\bar{I}(r')$ is the electric current distribution along the antenna, I_o is the current at the center of the dipole and γ is the angle between “ r' ” and the spherical vector “ \mathbf{r} ”. The current distribution along the antenna is determined by using the FEM. The polarization mismatch factor p is given by

$$p = \frac{|\bar{h} \cdot \bar{E}^i|^2}{|\bar{h}|^2 |\bar{E}^i|^2}, \quad 0 \leq P \leq 1 \tag{7}$$

The design of the good tag antenna comes down to the enhancement of the reflection coefficient Γ_{tag} , which is to get a good matching for the antenna impedance to the chip impedance. The reflection coefficient matching complex antenna port impedance to the complex chip impedance is given by [14]

$$\Gamma_{tag} = \frac{Z_c - Z_a^*}{Z_c + Z_a} \tag{8}$$

where $Z_c = R_c + jX_c$ is the chip impedance and $Z_a = R_a + jX_a$ is the antenna impedance. The most important tag performance characteristic is read range — the maximum distance at which RFID

reader can detect the backscattered signal from the tag. The tag read range was computed from Friis free-space formula as [19]

$$R = \frac{\lambda}{4\pi} \sqrt{\frac{P_t G_t G_r \tau p}{P_{th}}} \quad (9)$$

where λ is the wavelength, P_t is the power transmitted by the reader, G_t is the gain of the transmitting antenna, G_r is the gain of the receiving tag antenna, P_{th} is the minimum threshold power necessary to provide enough power to the RFID tag chip which is -10 dBm, P is the polarization mismatch factor and τ is power transmission coefficient given by

$$\tau = \frac{4R_c R_a}{|Z_c + Z_a|^2}, \quad 0 \leq \tau \leq 1 \quad (10)$$

The tag range bandwidth can be defined as the frequency band in which the tag offers an acceptable minimum read range over that band. A better than 95% power transmission coefficients can be achieved in the world UHF RFID band. Better matching and higher antenna gain is a straightforward and effective way to improve the tag reading range.

When the tag antenna is loaded with an IC chip which is a function of the input power and the operating frequency. The radar cross section, RCS, can be altered by terminating the antenna with chip impedances, the modulation depth of the RCS affects the tag reading range [19–22]. Generally the RCS of a tag antenna can be defined by

$$\sigma = \lim_{r \rightarrow \infty} 4\pi r^2 \frac{|\bar{E}^s|^2}{|\bar{E}^i|^2} \quad (11)$$

where \bar{E}^s is the total scattered field from loaded tag antenna. Through this paper, the finite element method (FEM) [23–26] is used to demonstrate the tag antenna performance.

3. NUMERICAL RESULTS

For reference purposes with available measurements, a fractal antenna dipole in free space [15] is investigated. Figure 2 shows a comparison between the measured values of the input impedance and the simulated results. The antenna used is 3rd-iteration Koch monopole with dimensions such as $L_a = 8$ cm, wire radius $a = 0.12$ mm and $\alpha = 60^\circ$. Good agreement is obtained. Fig. 3 shows the variations of the polarization mismatch factor and the magnitude of the open-circuit voltage against the operating frequency. To verify the fractal antenna

at any iteration is linearly polarized, the antenna is illuminated by a plane wave of circular polarization of right-hand sense in y - z plane. The value of the polarization mismatch factor is 0.5 and is constant with the frequency variation. The open circuit voltage changes from 58 mV to 29 mV in the RFID frequency range.

To electrically isolate the antenna from the object, it is assumed that the tag will be attached onto the object through a thin silicon-dioxide substrate. The tag antenna layout is shown in Figure 4. The tag antenna consists of fractal dipole sandwiched between two dielectric layers. The top and bottom layers are made of silicon-dioxide with dielectric constant of $\epsilon_{r1} = 4$, each of thickness 1.6 mm. The supersaturate layer is used to protect the antenna from the outer environment with the effect on the antenna performance [27]. The antenna has been designed and optimized using the finite element method. The design process involves as a first step a major tuning of the antenna input impedance, with the chip impedance, obtained by modifying the height L_a and the suspended angle α . The tag antenna has $2L_a = 7.58$ cm and $\alpha = 70^\circ$ etched in 0.018 mm copper with width $W_d = 1.4$ mm on a 3.2 mm silicon-dioxide substrate. The total dimension of the tag is $8.5 \times 2.14 \times 0.32$ cm³. The behavior of antenna input impedance, chip impedance, reflection coefficient, power transmission coefficient, and the read range as functions of frequency are illustrated in Figure 5. The maximum read range obtained is 4.76 m at 910 MHz corresponding to power transmission coefficient of 0.993 at the tag resonance frequency. The reflection coefficient of the antenna at 910 MHz is -49.86 dB and -10 dB bandwidth is 60 MHz (RFID UHF band is 902–928 MHz in North and South America). The simulated E -

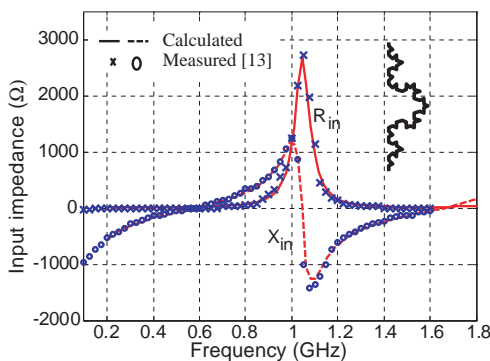


Figure 2. Input impedance of the 3rd-iteration Koch fractal monopole of length $L_a = 8$ cm and conductor radius $a = 0.012$ mm.

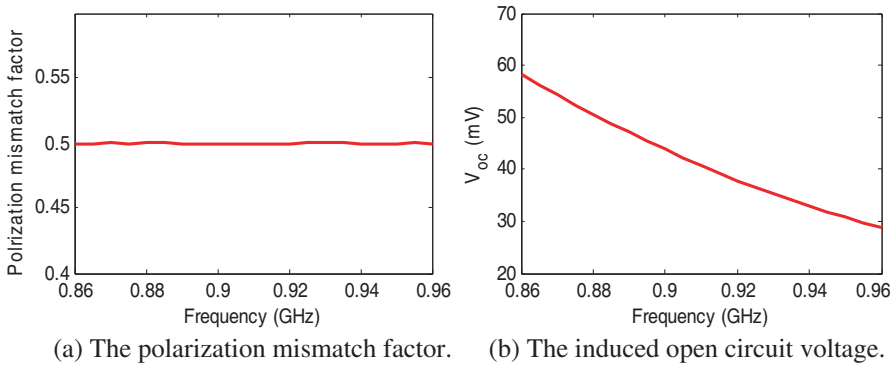


Figure 3. Variations of the polarization mismatch factor and the open circuit voltage against frequency of the fractal Koch monopole K_3 with $\alpha = 70^\circ$, $L_a = 8$ cm, and $a = 0.12$ mm.

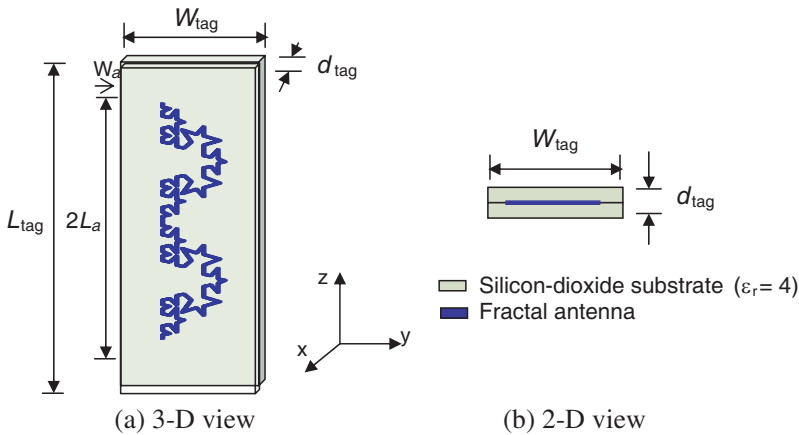


Figure 4. The tag antenna configuration with length L_{tag} , width W_{tag} and thickness d_{tag} .

and H -plane radiation patterns at $f = 910$ MHz for the tag antenna are shown in Figure 6. These curves show that the obtained radiation patterns are somewhat similar to that of a typical dipole. Omni-directional pattern in the H -plane is observed. Figure 7 shows the gain of the antenna versus the operating frequency.

In the backscattering-modulation process, the impedance of the IC chip is changed between two states. By changing the input impedance, the RCS of the tag and the power received by the reader are changed. The difference between radar cross sections of the two modulation

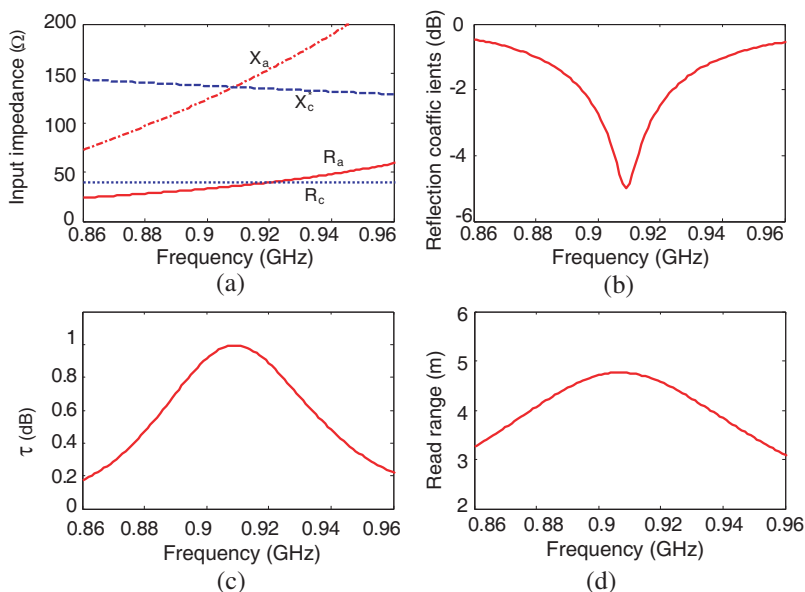


Figure 5. The properties of the tag antenna $8.5 \times 2.14 \times 0.32 \text{ cm}^3$ with $\alpha = 70^\circ$, $2L_a = 7.58 \text{ cm}$ and $W_a = 1.4 \text{ mm}$. (a) The tag antenna input impedance (R_a , X_a) and chip impedance (R_c , X_c^*). (b) The reflection coefficient. (c) The power transmission coefficient. (d) The tag antenna read range.

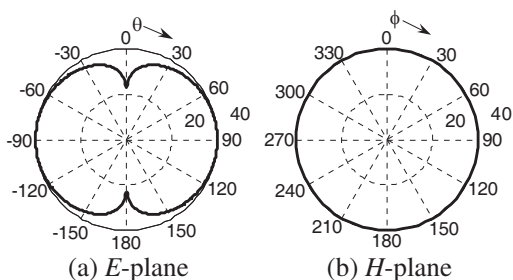


Figure 6. The E -plane and H -plane radiation pattern of the tag antenna of size $8.5 \times 2.14 \times 0.32 \text{ cm}^3$ with $\alpha = 70^\circ$, $2L_a = 7.58 \text{ cm}$ and $W_a = 1.4 \text{ mm}$ in free space.

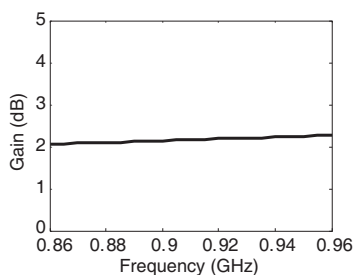


Figure 7. The tag antenna gain G versus frequency for tag antenna of size $8.5 \times 2.14 \times 0.32 \text{ cm}^3$ with $\alpha = 70^\circ$, $2L_a = 7.58 \text{ cm}$ and $W_a = 1.4 \text{ mm}$ in free space.

states is called the differential (or delta) RCS ($\Delta\sigma$). An incident plane wave traveling normal to the tag (x -direction) is used to excite the tag. The scattered field calculated with this load impedance represents the fields seen by the reader. Typically tags respond to the reader by either varying the amplitude of the backscattered fields (ASK modulation) or

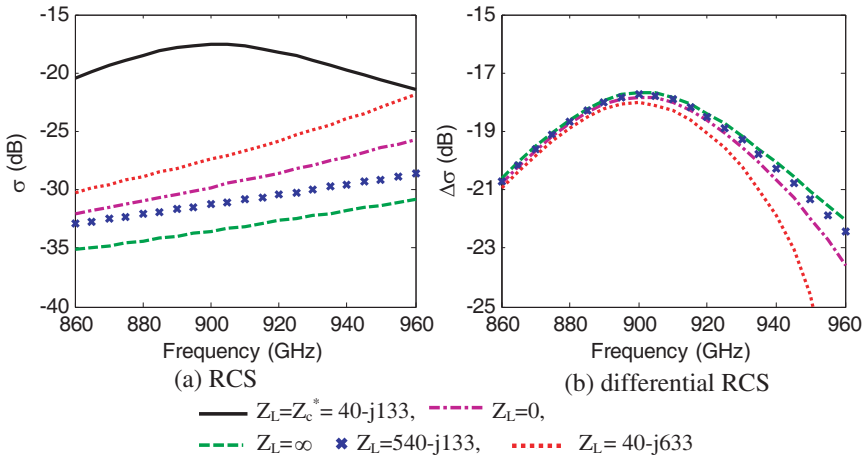


Figure 8. The RCS and differential RCS for tag antenna of size $8.5 \times 2.14 \times 0.32 \text{ cm}^3$ with $\alpha = 70^\circ$, $2L_a = 7.58 \text{ cm}$ and $W_a = 1.4 \text{ mm}$ in free space at different loads.

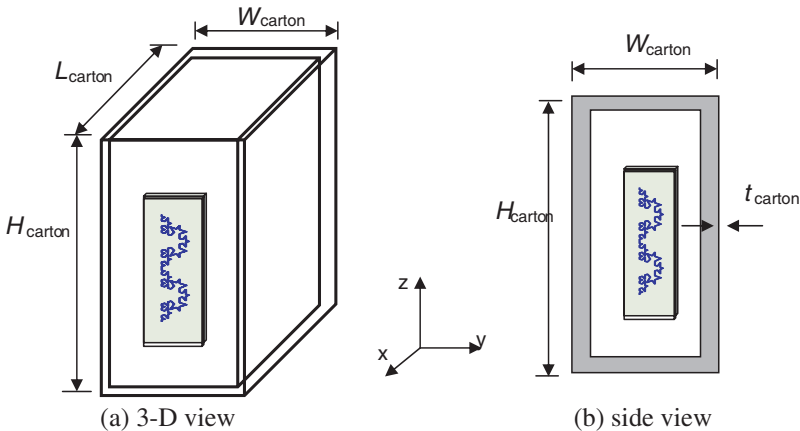


Figure 9. The tag antenna configuration over Carton box with length L_{carton} , width W_{carton} , height H_{carton} , and thickness t_{carton} , of simulated Carton material with $\epsilon_{r2} = 2$ and $\tan \delta = 0.04$.

the phase (PSK modulation). In the simulation the modulation is made by varying the real part (for ASK) or the imaginary part (for PSK) of the load impedance [28]. Figure 8(a) shows the radar cross section for the tag in free space against frequency. Different antenna loads are considered. Cases include chip impedance conjugate matching ($Z_L = 40 - j133$), short circuit ($Z_L = 0$), open circuit ($Z_L = \infty$), ASK modulation ($Z_L = 540 - j133$) to produce amplitude variation, and for PSK modulation ($Z_L = 40 - j633$) to give phase variation are considered [21]. Figure 8(b) shows the differential radar cross section “ $\Delta\sigma$ ” for the tag in free space against frequency. Different antenna loads are considered. Cases include ($Z_L = 0$), ($Z_L = \infty$), ($Z_L = 540 - j133$), and ($Z_L = 40 - j633$) are considered.

As the performance of the tag is influenced by the attached

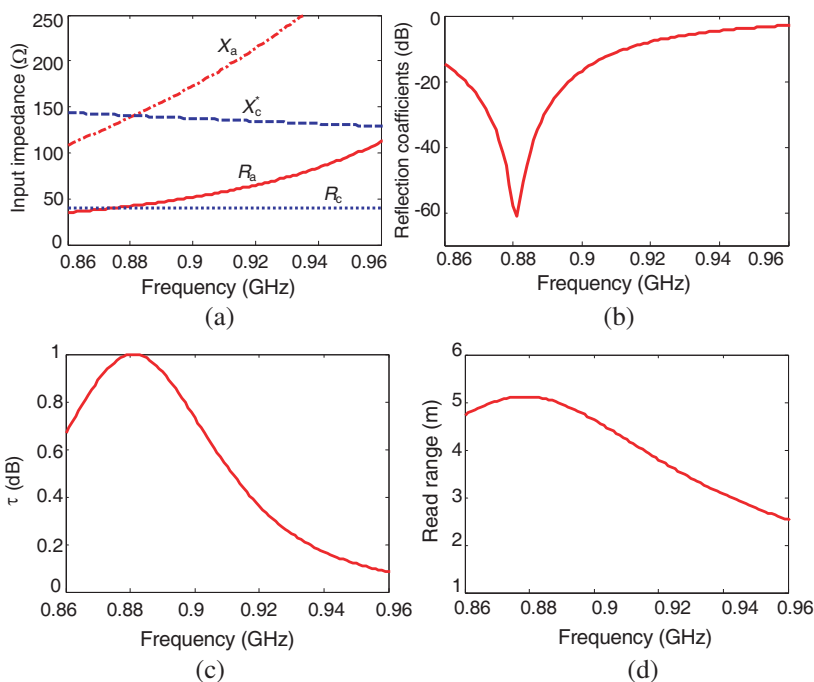


Figure 10. The tag antenna of size $8.5 \times 2.14 \times 0.32 \text{ cm}^3$ with $\alpha = 70^\circ$, $2L_a = 7.58 \text{ cm}$ and $W_a = 1.4 \text{ mm}$ placed over dielectric box of size $40 \times 40 \times 16.82 \text{ cm}^3$ with $\epsilon_{r2} = 2$ and $\tan \delta = 0.04$ with thickness 3 mm. (a) The tag antenna input impedance (R_a , X_a) and chip impedance (R_c , X_c^*). (b) The reflection coefficient. (c) The power transmission coefficient. (d) The tag antenna read range.

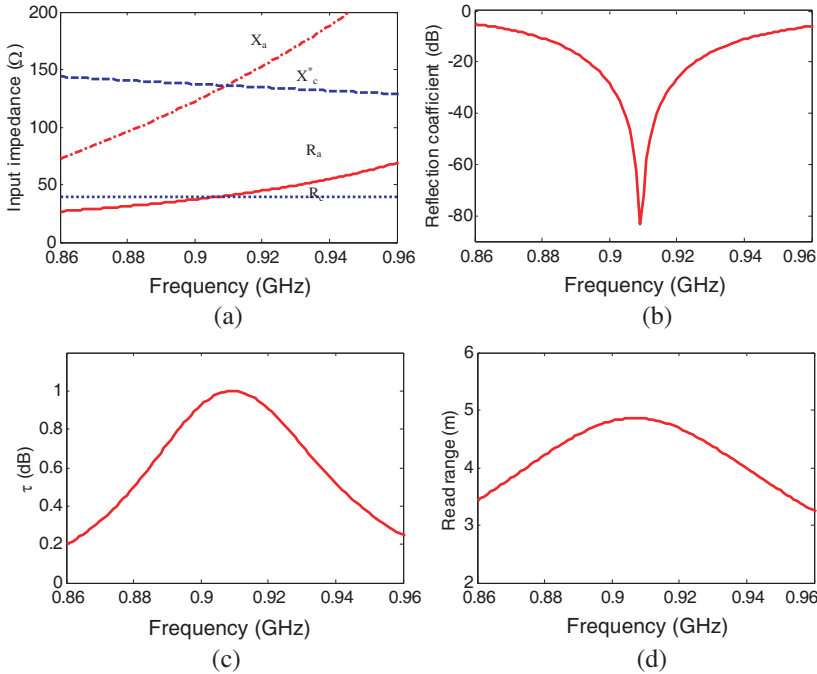


Figure 11. The tag antenna after re-design of size $8 \times 2.08 \times 0.32 \text{ cm}^3$ with $\alpha = 70^\circ$, $2L_a = 7.35 \text{ cm}$ and $W_a = 1.4 \text{ mm}$ placed over dielectric box of size $40 \times 40 \times 16.82 \text{ cm}^3$ with $\epsilon_r = 2$ and $\tan \delta = 0.04$ with thickness 3 mm. (a) The tag antenna input impedance (R_a , X_a) and chip impedance (R_c , X_c^*). (b) The reflection coefficient. (c) The power transmission coefficient. (d) The tag antenna read range.

object, this object is simulated as a dielectric box of dimension $H_{\text{carton}} \times L_{\text{carton}} \times W_{\text{carton}}$ equal $40 \times 40 \times 16.82 \text{ cm}^3$. The dielectric material is a simulation of Carton material with $\epsilon_{r2} = 2$, thickness $t = 3 \text{ mm}$ and $\tan \delta = 0.04$. Figure 9 shows the tag antenna placed over the dielectric box. The tag antenna input impedance, chip impedance, the power reflection coefficient, the power transmission coefficient, and the tag read range versus the operating frequency are illustrated in Figure 10. The tag antenna dimensions are as in Figure 5. The performance of the tag antenna is changed due to the effect of the dielectric box. Performance changes include shifted resonance frequency, and degraded impedance matching. Therefore, new tag antenna length $2L_a$ must be tuned through the design to remove the effect of the dielectric box. The new tag dimensions are

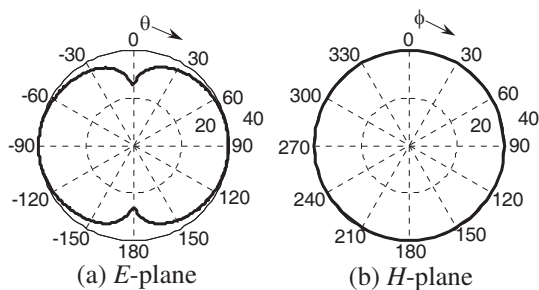


Figure 12. The *E*-plane and *H*-plane radiation pattern of the tag antenna over dielectric box of size $8 \times 2.08 \times 0.32 \text{ cm}^3$ with $\alpha = 70^\circ$, $2L_a = 7.35 \text{ cm}$ and $W_a = 1.4 \text{ mm}$ placed over dielectric box of size $40 \times 40 \times 16.82 \text{ cm}^3$ with $\epsilon_{r2} = 2$ and $\tan \delta = 0.04$ with thickness 3 mm.

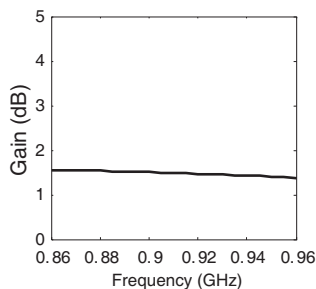


Figure 13. The tag antenna gain G verses frequency for tag antenna of size $8 \times 2.08 \times 0.32 \text{ cm}^3$ with $\alpha = 70^\circ$, $2L_a = 7.35 \text{ cm}$ and $W_a = 1.4 \text{ mm}$ over dielectric box of size $40 \times 40 \times 16.82 \text{ cm}^3$ with $\epsilon_r = 2$ and $\tan \delta = 0.04$ with thickness 3 mm.

$8 \times 2.08 \times 0.32 \text{ cm}^3$, with $2L_a = 7.35 \text{ cm}$ and $W_a = 1.4 \text{ mm}$. The performances of tag antenna on the dielectric box are depicted in Figure 11. The corresponding *E*-plane and *H*-plane radiation pattern at 910 MHz and the tag antenna gain versus the operating frequency are shown in Figure 12 and Figure 13 respectively.

An object with length $L_{\text{object}} = 29.4 \text{ cm}$, width $W_{\text{object}} = 6.28 \text{ cm}$ and height $H_{\text{object}} = 29.4 \text{ cm}$ with dielectric permittivity ϵ_{r3} is placed on the center of the dielectric box and the tag antenna is attached to the dielectric box as shown in Figure 14. The object is made from different materials includes (1) Arlon AD 320 (tm) with $\epsilon_{r3} = 3.2$ and dielectric loss $\tan \delta = 0.003$ (object1), (2) glass with $\epsilon_{r3} = 5.5$ (object2), and (3) copper with $\sigma = 5.8 \times 10^8 \text{ s/m}$ (object3). The performance of the tag in the presence of the dielectric box and different object

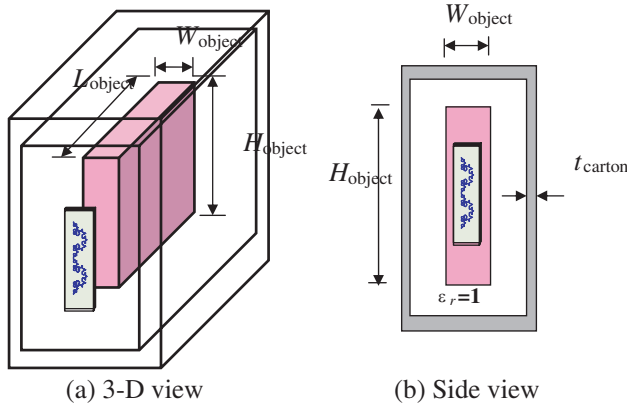


Figure 14. The tag antenna configuration over carton box with the object placed on its center. The object dimensions $L_{\text{object}} \times W_{\text{object}} \times H_{\text{object}} = 29.4 \times 29.4 \times 6.28 \text{ cm}^3$ of different materials.

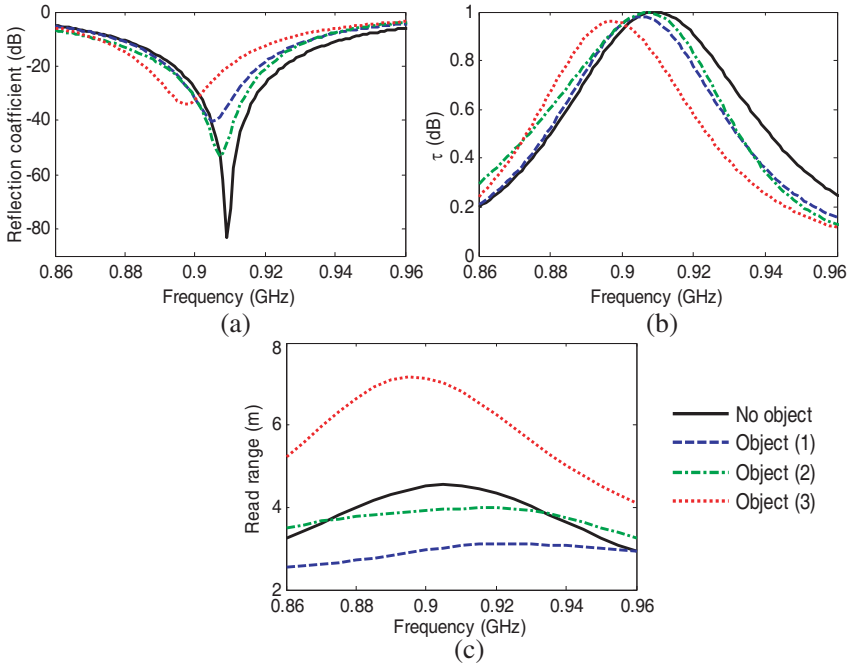


Figure 15. The tag antenna attached to carton box contains different objects. (a) The reflection coefficient, (b) The power transmission coefficient, (c) The tag antenna read range.

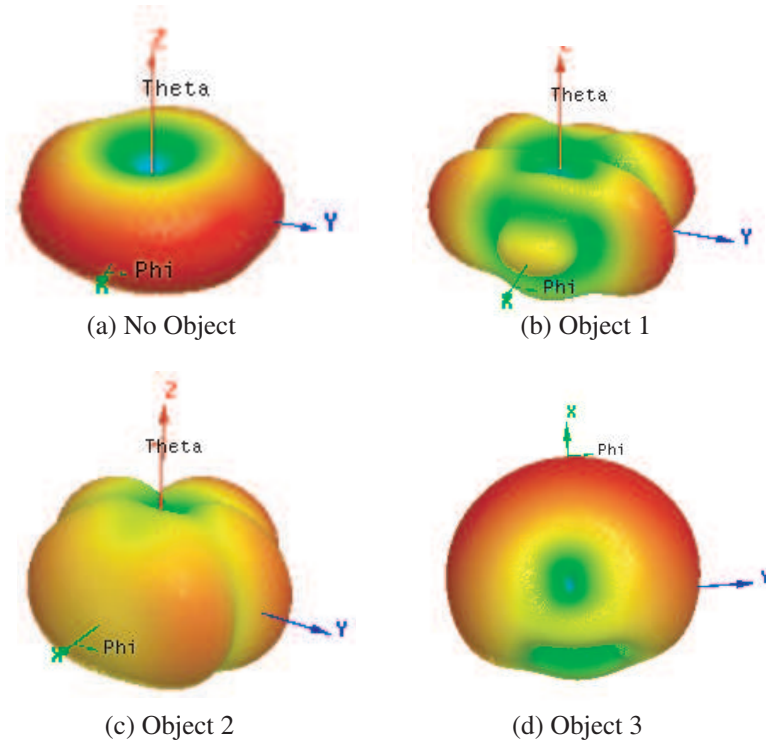


Figure 17. The 3-D radiation pattern of the tag antenna attached to Carton box containing different objects.

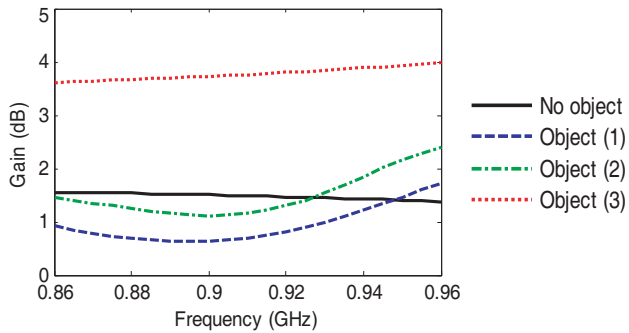


Figure 18. The tag antenna gain G verses frequency for tag antenna attached to Carton box containing different objects.

Table 1. The performance of the tag antenna in the presence of carton box and objects.

Tag parameters	No Object	(Object 1)	(Object 2)	(Object 3)
f_o (GHz)	0.910	0.905	0.907	0.897
Γ_{\min} (dB)	-49.86	-40.34	-53.32	-34.04
BW (MHz)	60	55	62	53
τ_{\max}	0.993	0.98	0.99	0.96
R_{\max} (m)	4.76	3.12	3.988	7.225

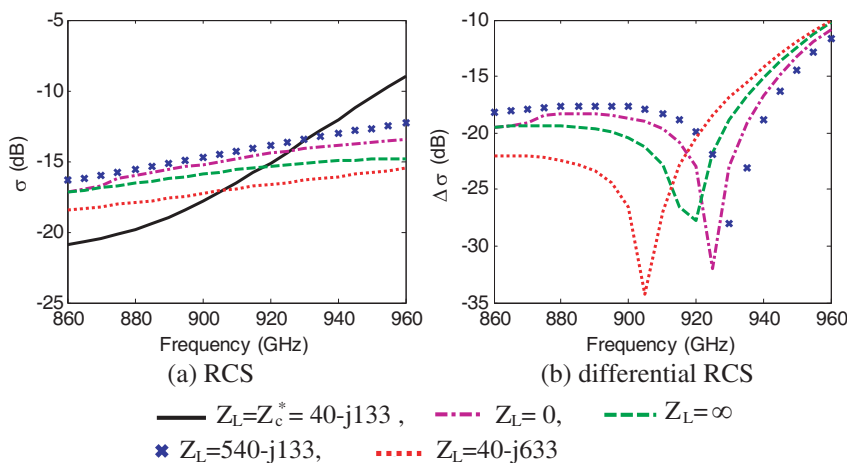


Figure 19. The RCS and differential RCS for tag antenna of size $8 \times 2.08 \times 0.32 \text{ cm}^3$ with $\alpha = 70^\circ$, $2L_a = 7.35 \text{ cm}$ and $W_a = 1.4 \text{ mm}$ placed over dielectric box of size $40 \times 40 \times 16.82 \text{ cm}^3$ with $\epsilon_r = 2$ and $\tan \delta = 0.04$ with thickness 3 mm, with the Arlon AD 320 (tm) object of size $29.4 \times 29.4 \times 6.28 \text{ cm}$ and $\epsilon_r = 3.2$, $\tan \delta = 0.003$ loaded with different chip impedances.

According to these cases the effect of the objects placed in the center of the dielectric box didn't have a significant effect on the performance of the tag antenna; there is a small shift in the resonance frequency but still within the operating frequency band. Also, the chip impedance matching change according to the object material properties. Both the power transmission coefficients and the read range change with the object material. The radiation pattern characteristics are affected by the presence of the object, but almost omni-directional patterns in

the H -plane are observed. Figure 18 shows the RCS and differential RCS for conjugated-matched antenna, loaded with $Z_L = 40 - j133 \Omega$, $Z_L = 0 \Omega$, $Z_L = \infty \Omega$, $Z_L = 540 - j133 \Omega$ and $Z_L = 40 - j633 \Omega$.

4. CONCLUSION

A fractal dipole antenna for passive UHF RFID applications has been proposed, analyzed and designed. The tag antenna consists of a modified Koch fractal dipole antenna sandwiched between two dielectric layers. The tag antenna has been designed and optimized using the finite element method. The proposed tag antenna can operate at 910 MHz. The antenna is simple and has good impedance matching with the chip impedance. The variation of the magnitude of the open-circuit voltage and the polarization mismatch factor against the operating frequency are explained. The input impedance, reflection coefficient, the power transmission coefficient and the read range are investigated. The RCS and differential RCS are calculated for different load impedances. There is a small shift in the resonance frequency due to the different objects placed inside the dielectric box around 13 MHz.

ACKNOWLEDGMENT

The authors would like to thank Prof. Dr Ahmed Kishk for valuable discussions, The authors are also grateful to the technical reviewers of the paper for their helpful comments.

REFERENCES

1. Chen, Z. N., *Antennas for Portable Devices*, Chapter 3, John Wiley & Sons, Ltd., UK, 2007.
2. Chen, S.-Y. and P. Hsu, "CPW-fed folded-slot antenna for 5.8 GHz RFID tags," *Electronic Lett.*, Vol. 24, 1516–1517, Nov. 2004.
3. Padhi, S. K., N. C. Karmakar, C. L. Law, and S. Aditya, "A dual polarized aperture coupling circular patch antenna using a C-shaped coupling slot," *IEEE Trans. Antennas Propag.*, Vol. 51, No. 12, 3295–3298, Dec. 2003.
4. Marrocco, G., "Gain-optimized self-resonant meander line antennas for RFID applications," *Antennas Wireless Propag. Lett.*, Vol. 2, No. 21, 302–305, 2003.
5. Hirvonen, M., P. Pursula, K. Jaakkola, and K. Laukkanen, "Planar inverted-F antenna for radio frequency identification," *Electronic Lett.*, Vol. 40, 848–850, Jul. 2004.

6. Qing, X.-M. and N. Yang, "A folded dipole antenna for RFID," *Proc. IEEE Antennas and Propagation Soc. Int. Symp.*, Vol. 1, 97–100, Jun. 2004.
7. Foster, P. R. and R. A. Burberry, "Antenna problems in RFID systems," *Proc. Inst. Elect. Eng. Colloquium RFID Technology*, 3/1–3/5, Oct. 1999.
8. Tan, K. G., A. R. Wasif, and C.-P. Tan, "Objects tracking utilizing square grid RFID reader antenna network," *Journal of Electromagnetic Waves and Applications*, Vol. 22, No. 1, 27–38, 2008.
9. Shi, X., F. Wei, Q. Huang, L. Wang, and X.-W. Shi, "Novel binary search algorithm of backtracking for RFID tag anti-collision," *Progress In Electromagnetics Research B*, Vol. 9, 97–104, 2008.
10. Li, X., L. Yang, S.-X. Gong, Y.-J. Yang, and J.-F. Liu, "A compact folded printed dipole antenna for UHF RFID reader," *Progress In Electromagnetics Research Letters*, Vol. 6, 47–54, 2009.
11. Best, S. R., "On the performance properties of the Koch fractal and other bent wire monopoles," *IEEE Trans. Antennas Propag.*, Vol. 51, No. 6, 1292–1300, Jun. 2003.
12. Seshagiri Rao, K. V., P. V. Nikitin, and S. F. Lam, "Antenna design for UHF RFID tags: A review and a practical application," *IEEE Trans. Antennas Propag.*, Vol. 51, No. 12, 3870–3876, Dec. 2005.
13. Nikitin, P. V. and K. V. S. Rao, "Theory and measurement of backscattering from RFID tags," *IEEE Antennas Propag. Mag.*, Vol. 48, 212–218, Dec. 2006.
14. Loo, C.-H., K. Elmahgoub, F. Yang, A. Elsherbeni, D. Kajfez, A. Kishk, and T. Elsherbeni, "Chip impedance matching for UHF RFID tag antenna design," *Progress In Electromagnetics Research*, PIER 81, 359–370, 2008.
15. Baliarda, C. P., J. Romeu, and A. Cardama, "The Koch monopole: A small fractal antenna," *IEEE Trans. Antennas Propag.*, Vol. 48, No. 11, 1773–1781, Nov. 2000.
16. Da Costa, K. Q. and V. Dmitriev, "Theoretical analysis of a modified Koch monopole with reduced dimensions," *IEE Proc. - Microw. Antennas Propag.*, Vol. 153, No. 5, 475–479, Oct. 2006.
17. Wunsch, A. D., "The vector effective length of slot antennas," *IEEE Trans. Antennas Propag.*, Vol. 39, No. 5, 705–709, May 1991.
18. Zainud-Deen, S. H., "Polarization losses in normal mode helical antenna," *1995 IEEE/AP-S International Symposium and*

- USNC/URSI Radio Science Meeting*, California, 1883–1886, 1995.
19. Fuschini, F., C. Piersanti, F. Paolazzi, and G. Falciasecca, “Analytical approach to the backscattering from UHF RFID transponder,” *Antennas Wireless Propag. Lett.*, Vol. 53, No. 12, 33–35, 2008.
 20. Pursula, P., D. Sandstrom, and K. Jaakkola, “Backscattering-based measurement of reactive antenna input impedance,” *IEEE Trans. Antennas Propag.*, Vol. 56, No. 2, 469–474, Feb. 2008.
 21. Penttila, K., M. Keskilammi, L. Sydanheimo, and M. Kivikoski, “Radar cross-section analysis for passive RFID systems,” *IEE Proc. - Microw. Antennas Propag.*, Vol. 153, No. 1, Feb. 2006.
 22. Youla, D. C., “On scattering matrices normalized to complex port numbers,” *Proc. I. R. E.*, Vol. 49, 12–21, Jul. 1961.
 23. Dong, X. and T. An, “A new FEM approach for open boundary Laplace’s problem,” *IEEE Trans. Microw. Theory Tech.*, Vol. 44, 157–160, Jan. 1996.
 24. Zhou, X. and G. W. Pan, “Application of physical spline finite element method (PSFEM) to full wave analysis of waveguide,” *Progress In Electromagnetics Research*, PIER 60, 19–41, 2006.
 25. Gavrilovic, M. M. and J. P. Webb, “Accuracy control in the optimization of microwave devices by finite element methods,” *IEEE Trans. Microw. Theory Tech.*, Vol. 50, No. 8, 1901–1911, Aug. 2002.
 26. Polycarpou, A. C., *Introduction to Finite Element Method in Electromagnetics*, Morgan & Claypool Publishers’ series, USA, 2006.
 27. Garg, R., P. Bhartia, I. Bahland, and A. Ittipiboon, *Microstrip Antenna Design Handbook*, Artech House, Inc., Norwood, USA, 2001.
 28. Johanson, J. and R Sainati, “Investigation of UHF RFID tag backscatter,” *Proc. IEEE Antennas and Propagation Soc. Int. Symp.*, Vol. 1, 2753–2755, Jun. 2007.